Heliyon 9 (2023) e19904

Contents lists available at ScienceDirect

Heliyon

journal homepage: www.cell.com/heliyon

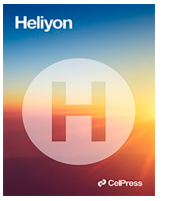

Application of co-precipitated glutinous rice starch as a multifunctional excipient in direct compression tablets

Chonticha Amornrojvaravut, Jomjai Peerapattana *

Division of Pharmaceutical Technology, Faculty of Pharmaceutical Sciences, Khon Kaen University, Khon Kaen, Thailand

A R T I C L E I N F O

Keywords:
Glutinous rice starch
Co-precipitated method
Direct compression
Co-precipitated glutinous rice starch
Pharmaceutical excipients
Tablets

A B S T R A C T

Two key properties of excipients for inclusion in direct compression tablets are flowability and compactibility. Glutinous rice starch (GRS) has poor flowability, which limits its use in direct compression tablets. This study aimed to create a multifunctional direct compression excipient (filler binder disintegrant) with improved flowability from GRS by the co-precipitation method. The physicochemical and pharmaceutical properties of the co-precipitated GRS (cpGRS) were investigated. The optimum conditions for producing cpGRS (0.43 M sodium hydroxide solution, 7.09% PVP K30, 14.02% calcium carbonate, 95 min of mixing time and pH of 6.97) resulted in 68.80% yield, fair to good flowability, acceptable tablet strength, and fast disintegration. The FT-IR spectra of cpGRS showed no significant shifts in the key peaks, which indicates that there was an absence of chemical interactions within cpGRS. X-ray diffractograms also showed no significant changes, indicating that the GRS granules, calcium carbonate, and PVP K30 components remained unaltered during co-precipitation. cpGRS also demonstrated a dilution capacity of 50% when paracetamol was used as model drug. When cpGRS was combined with domperidone or propranolol hydrochloride it showed a better deformation capability than the physical mixtures. Although cpGRS was sensitive to lubricant, the hardness and tensile strength were higher than common strength for general purpose use in tablets. When compared to the physical mixture, pregelatinized starch and directly compressible calcium carbonate, the results showed that cpGRS tablets of both model drugs passed the friability test, demonstrated the best disintegration property, provided the fastest and highest drug release profile for propranolol, and improved the drug release profile for domperidone. For propranolol-cpGRS tablets, dissolution medium at different pH did not affect the dissolution profile. For domperidone-cpGRS tablets, the pH of dissolution medium did affect the dissolution profile of the tablets. This was according to the API solubility. These results reveal that cpGRS is an excellent multifunctional i.e., filler, binder, and disintegrant excipient suitable for direct compression tablets. The main component is natural. The preparation method is simple, quick, and efficient. This method does not produce harmful waste and requires only basic equipment, and affordable reactants and devices.

1. Introduction

There are several ways to prepare a tablet. The direct compression method has many advantages over wet and dry granulation in that it uses fewer steps and requires fewer units to operate, and it has lower labor costs, shorter operating times, and lower energy

* Corresponding author.
E-mail address: jomsuj@kku.ac.th (J. Peerapattana).

https://doi.org/10.1016/j.heliyon.2023.e19904
Received 19 April 2023; Received in revised form 5 September 2023; Accepted 5 September 2023
Available online 6 September 2023

consumption. However, direct compression methods require excipients with good flowability, compactibility, disintegration ability, and particle size uniformity [1].

Glutinous rice starch (GRS) has many desirable excipient properties. It is cheap, renewable, biodegradable, and has acceptable binding and disintegrating properties. However, its poor flowability and compactibility properties remain a limitation for tableting processes. The flowability of GRS is rated as very poor to fair [2,3]. Tablets prepared from GRS have lower hardness than those prepared from corn starch at similar concentrations [3].

There are many methods that can be used to improve the excipient properties of starch but, when one property is improved, another property may be impaired [4–7]. For instance, the flowability of Avicel® PH-200 was increased at the cost of decreased tablet hardness compared to Avicel® PH-101 [4]. The co-processed method is a physical modification method used to combine two or more excipients together that results in the excipients retain their chemical characteristics while more benefits than can be obtained by simple physical mixing of the excipient components. Previous studies have co-processed corn starch with lactose [8], microcrystalline cellulose [9], acacia gum [10], and potato starch [11] in order to improve flowability, compactibility, crushing strength or hardness, disintegration, release profile, and loading capacity. Co-processing of rice starch and microcrystalline cellulose also showed good compressibility [12]. However, to our knowledge, there are no previous reports investigating co-processed GRS.

The co-precipitated method is a co-processed method that can modify pharmaceutical excipients easily, rapidly, and effectively. This method uses simple tools, inexpensive reactants and devices, and does not generate toxic waste. Rice starch co-precipitated with colloidal silicon dioxide showed good flowability and compactibility [13]. Corn starch co-precipitated with magnesium silicate showed rapid disintegrant properties, high compressibility and compactibility with low lubricant sensitivity [14]. Thus, co-precipitated excipients have potential for development as multifunctional excipients in tablet formulations.

The deformation (compressibility) and bonding (compactibility) behavior of powder under stress has the greatest influence on the tabletting of powder [15]. While compactibility addresses the formation of solid compacts under pressure, compressibility refers to a powder's ability to densify under pressure. When compressing brittle materials like sucrose, lactose, or silicon dioxide, the stresses within the particles increase and cause fragmentation. This increases the number of particles and results in the formation of new, clean surface bonding. For plastic materials such as polyvinyl pyrrolidone, crospovidone, maize starch, guar gum, and sorbitol, fragmentation under compression does not take place. The change in particle shape caused by groups of particles sliding is known as plastic deformation. The type of deformation is influenced by the material's physical characteristics as well as the intensity and rate of the applied force, and how long the pressure was applied locally. The stress within the particles rises as a result of the material's resistance to deformation. The particles deform elastically, or reversibly, if the applied stress is removed before the deformation reaches a particular critical value. As a result, the particles inside the powder bed resume their original form. If the pressure is over the critical value, the powder bed deforms plastically, meaning that releasing the applied pressure will have no effect on the deformed particles. The particles will continue to be in their deformed state, which is compaction. When a deforming force is removed in case of a viscoelastic flow (such as MCC and hydroxyl methyl cellulose), it will revert to its previous shape [16]. Thus, perfect diluents should be a combination of both brittle and plastic materials that fragment and deform to combine the benefits of both materials.

This study aimed to overcome the flowability and compactibility limitations of GRS by employing the co-precipitated method. Central composite design (CCD) was used to identify the optimal conditions to obtain the proper co-precipitated excipient. Polyvinyl pyrrolidone k30 (PVP K30), a plastic deformed material, and calcium carbonate, a brittle deformed material, were co-precipitated with GRS, a plastic-elastic deformed material [17,18], in order to generate a synergistic effect on flowability and compactibility. Both co-precipitating substances are commonly used as binder and filler, respectively, in tablet dosage form. The physicochemical properties of the co-precipitated GRS (cpGRS) i.e., powder flowability, molecular interaction, moisture content, crystalline structure, dilution potential, lubricant sensitivity and surface morphology were compared with the model excipients pregelatinized starch (PGS) and directly compressible calcium carbonate (CS90). The effect of an active pharmaceutical ingredient (API)'s solubility on the pharmaceutical properties of cpGRS tablets was also investigated.

2. Materials and methods

2.1. Materials

Glutinous rice starch (GRS, General Food Products, Thailand), polyvinyl pyrrolidone k30 (PVP K30, Ashland, Calvert City, USA) and calcium carbonate light (Konoshima Chemical, Osaka, Japan) were used to prepare cpGRS. Magnesium stearate (Faci Asia Pacific, Singapore) was used as lubricant. Propranolol hydrochloride (Ipca Laboratories, India) was used as a soluble model drug. Domperidone (Sri Krishna Pharmaceuticals, India) was used as an insoluble model drug. Paracetamol (Anqiu Lu'an Pharm., China) was used as a poorly compactable model drug. Pregelatinized starch (National 78–1551, Ingredion, Germany) and directly compressible calcium carbonate (Barcroft™ CS90, SPI Pharma, Germany) were used as model excipients. All chemical substances used in this study were of pharmaceutical grade.

2.2. Methods

2.2.1. The experimental design

Central composite design (Design-Expert® version 13, Statease, Minneapolis, USA) was selected to design the experiment. There were five interested variables: the concentration of sodium hydroxide solution (X_1, 0.0–0.6 M), the mixing time (X_2, 60–180 min), the pH at endpoint (X_3, 2–9), the amount of PVP K30 (X_4, 0–10% w/w), and the amount of calcium carbonate (X_5, 0–20% w/w),

Supplementary file 1. The interesting responses were the percentage yield (Y_1), Carr's index (Y_2) and the Hausner ratio (Y_3), which were calculated from tapped and bulk densities, the tensile strength (Y_4) and the disintegration time (Y_5). A total of 47 experiments, including five repeating at the center points, were conducted. The optimal composition and conditions that provided the proper cpGRS, i.e., highest percentage yield and tensile strength, and lowest Carr's index, Hausner ratio, and disintegration time, were selected using the desirability function.

2.2.2. Preparation of cpGRS

GRS (300 g) was dispersed in 600 ml. of 0.05 M NaOH solution and stirred with a magnetic stirrer until homogenous. The additives, 7.09% PVP K30 (X_4), and 14.02% Calcium carbonate (X_5), were dispersed in another 600 ml. of 0.43 M NaOH solution (X_1) and stirred with a magnetic stirrer until homogenous. The additive suspension was mixed with the starch suspension and stirred for 95 min (X_2). After mixing, hydrochloric acid solution (2 M) was added into the mixture until the pH of the mixture reached 6.97 (X_3), which reversed the swelling of starch granules and resulted in precipitation of cpGRS. A nylon sheet was used to filter the cpGRS and distilled water was used to wash the products and remove the salts. The cpGRS was dried at 50 °C for 48 h in a hot air oven and ground with mill grinder. The products were kept in desiccator until use.

2.2.3. Physicochemical properties of cpGRS

2.2.3.1. The percentage yield, powder flowability and moisture content. The percentage yield is the percent ratio of experimental yield to theoretical yield, Equation (1) [19]. The experimental yield represents the actual amount of cpGRS obtained during a specific experiment, while the theoretical yield refers to the total weight of GRS, calcium carbonate, and PVP K30 that would be obtained without any process losses.

$$\text{Percent yield} = \frac{\text{Experimental yield}}{\text{Theoretical yield}} \times 100 \tag{1}$$

The bulk and tap densities were calculated from the mass of starch powder and the volume before and after tapping, until the final volume remained unchanged, respectively, (Equation (2) and (3)). The Hausner ratio was calculated from the proportion of the tapped density to the bulk density, Equation (4). Carr's index was the percentage ratio of the difference between the tapped and bulk densities to the tapped density, Equation (5). The Hausner ratio and Carr's index are commonly used to identify powder flowability [19]. The average and standard deviation (S.D.) of three investigations was calculated.

$$\text{Bulk density} = \frac{\text{Mass of powder}}{\text{Bulk volume}} \tag{2}$$

$$\text{Tapped density} = \frac{\text{Mass of powder}}{\text{Tapped volume}} \tag{3}$$

$$\text{Hausner ratio} = \frac{\text{Tapped density}}{\text{Bulk density}} \tag{4}$$

$$\text{Carr's index} = \left(1 - \frac{\text{Bulk density}}{\text{Tapped density}}\right) \times 100 \tag{5}$$

The moisture content was measured using an electrical moisture analyzer (Aczet MB50, Piscataway, USA). The temperature was set at 105 °C. The sample (5 g) was put on the pan and the exact weights of the sample were recorded before and after heating to a constant weight and then used for calculating the moisture content.

2.2.3.2. The molecular interaction and crystalline structure. The presence of functional groups and the molecular interactions of each substance were analyzed by Fourier-transform infrared (FT-IR) spectrophotometer (Spectrum One, PerkinElmer, Norwalk, USA) using the KBr disk method. Samples (cpGRS, GRS, PVP K30, and calcium carbonate) were crushed with KBr pellets before being pressed as a disk using a hydraulic press at 10 tons for 10 min. The disk was then put in a sample holder and scanned from 4000 to 400 cm^{-1} at a resolution of 4 cm^{-1}. The absorbance peaks of cpGRS, GRS, PVP K30 and calcium carbonate were recorded.

cpGRS, GRS, PVP K30 and calcium carbonate were investigated for their crystallinity and polymorphism using a Powder X-ray diffractometer (Bruker D2 phaser diffractometer, Bruker, USA). The Bragg Angle (2θ) range of diffractograms of 5–80° at a scan rate of 0.5 s per step and a step size of 0.02° were set.

2.2.3.3. The surface morphology and particle size distribution. cpGRS, GRS, PVP K30 and calcium carbonate were attached with carbon tape and coated with gold to make the samples conductive. Photomicrographs of all samples were taken by scanning electron microscopy (Hitachi SU3800, Tokyo, Japan) at various magnifications to examine the surface morphology.

A laser diffraction particle size analyzer (Mastersizer2000 Model Hydro2000SM, Malvern Instrument, UK) was used to determine the particle size distribution. Five-gram samples were placed into the sample holder. The volume weighted mean was used to express particle size and the measurement was taken in triplicate.

2.2.4. cpGRS tablet preparation

cpGRS 320 mg tablets were prepared by a hydraulic press machine (Kobata gauge MFG., Japan) at compaction pressure of 214.56 MPa equipped with flat faced punches 10 mm in diameter. Tablets were kept 24 h in desiccator before testing.

2.2.4.1. Disintegration time. The disintegration time of cpGRS tablets was investigated by using a disintegration apparatus (Erweka ZT 324, Langen, Germany) and water at 37 ± 0.5 °C as the disintegrating medium. The average and S.D. of six tablets were calculated.

2.2.4.2. The tensile strength. A hardness tester (Erweka TBH 125, Langen, Germany) was used to determine the hardness of cpGRS tablets. The tensile strength was calculated from Equation (6). Where F is the force required to cause failure in tension (N), π is a mathematical constant, D is the diameter of the tablets (cm) and h is the thickness of the tablets (cm) [3]. The average and S.D. of six tablets were calculated.

$$\text{The tensile strength} = \frac{2F}{\P Dh} \tag{6}$$

2.2.5. Dilution potential of cpGRS

This experiment measures the proportion of a poorly compactable drug that can be incorporated into an excipient and still provide satisfactory tablets. cpGRS and paracetamol were mixed at various concentrations (0%, 10%, 20%, 30%, 40%, 50%, 60%, and 70%) in a mixer for 10 min. Then 0.75% magnesium stearate was added and mixed for an additional 5 min. The tablets were prepared using a hydraulic press machine at 143.04, 178.80, 214.56, 286.09, and 357.61 MPa of compaction pressure equipped with flat faced punches 10 mm in diameter with 320 mg/tab. The tablets were kept for 24 h before measuring the hardness. The tensile strength/compaction profile equation is shown in Equation (7).

$$\sigma_t = a\,P^2 + bP + c \tag{7}$$

where σ_t is the tensile strength (MPa), P is the compaction pressure (MPa), and a, b and c are constants. The integration equation in the limits of compaction pressure, P1 to P2 with the area under the curve (AUC), as function of compaction pressure, is shown in Equation (8).

$$AUC = \frac{aP^3}{3} + \frac{bP^2}{2} + cP + d \tag{8}$$

The AUC of each mixture was divided by the AUC of 0% w/w mixture to give the ratio known as work potential or area ratio. This area ratio was plotted against the % w/w of paracetamol. The linear regression which extrapolated to zero area ratio is the value of the dilution capacity [20].

2.2.6. Lubricant sensitivity

For lubricant sensitivity testing, 100 g. of cpGRS and a physical mixture (PM) of the same components and standard excipients (i.e., PGS and CS90) were separately mixed with magnesium stearate at 0.1, 0.5, 1, 3, and 5% w/w for 5 min. The tablets were compressed using a hydraulic press tableting machine equipped with flat faced punches 10 mm in diameter with 320 mg/tab, at 214.56 Mpa compaction pressure. The tablets were kept for 24 h before measuring the tablet hardness.

The lubricant sensitivity is shown as lubricant sensitivity ratio (LSR). This ratio represents the hardness of tablets with and without lubricant, which is calculated by Equation (9).

$$\text{LSR} = \left(\frac{S_0 - S_{lub}}{S_0}\right), \tag{9}$$

where S_0 and S_{lub} are the hardness of tablets without and with a lubricant, respectively [21].

2.2.7. Medicated tablet preparation

Medicated tablets were prepared by the direct compression method using a hydraulic press tableting machine equipped with flat-faced punches 8 mm in diameter with 133 mg/tab, at 335.26 Mpa of compaction pressure. The model drugs, domperidone (as insoluble model drug) and propranolol hydrochloride (as soluble model drug), made up 30% of the tablets' weight, along with excipients (cpGRS, PM, PGS and CS90) and 0.75% of magnesium stearate. All medicated tablets were kept for 24 h before measuring the tablet properties as described in 2.2.8.

2.2.8. Pharmaceutical properties of the medicated tablets

2.2.8.1. The tablet strength and friability. The hardness tester *(*Erweka TBH 125, Langen, Germany*)* was used to determine the hardness. The average and S.D. of six tablets was calculated.

Samples of whole tablets were taken as near as possible to 6.5 g and the dust was removed. The tablets were weighed and put into a drum and rotated at a speed of 25 rpm for 4 min. After that, the tablets were withdrawn, any dust was removed and the whole tablet was weighed. The difference in weight before and after testing must be equal to or less than 1% to meet the requirement [22].

2.2.8.2. In vitro disintegration time. The *in vitro* disintegration time of the tablets were evaluated by the same method described in 2.2.4.1.

2.2.8.3. Dissolution testing. The dissolution test of propranolol tablets was performed by USP apparatus 1 *(*basket apparatus*)* with a rotation speed of 100 rpm [2]. USP apparatus 2 *(*paddle apparatus*)* was used at a rotation speed of 50 rpm for domperidone tablets [23]. A variety of media were used i.e., *(1)* 0.1 N HCl *(*pH 1.2*)*, *(2)* acetate buffer *(*pH 4.5*)*, and *(3)* phosphate buffer *(*pH 6.8*)* at the temperature of 37 ± 0.5 °C [24]. Media samples were collected at 2, 5, 10, 15, 30, 45, 60, 90, and 120 min and replaced with an equal volume of fresh medium. The filtered samples were assayed by a UV–Visible spectrophotometer, in which domperidone was analyzed at the wavelength of 284 nm [23] and propranolol hydrochloride at the wavelength of 289 nm [2]. The percentages of drug release were calculated and plotted against time to create a dissolution profile for each medicated tablet. Each dissolution test was performed in triplicate.

2.2.8.4. Compactibility of cpGRS. Tablets, with the same composition as those prepared in 2.2.7, were compacted by using a hydraulic press at compaction pressures of 111.75, 167.63, 223.50, 279.38, and 335.26 MPa. The hardness tester was used to determine the hardness of six tablets. The mean of hardness and the standard deviation were plotted against compaction pressures to calculate pressure hardness profiles (PHP). The compactibility of the sample powders was determined from the slope of PHP and the hardness range of the compacts. The plastic deformation of the tablets was determined from the Heckel equation (Equation (10)).

$$\ln \frac{1}{1-D} = PK + A \tag{10}$$

Where P is the compaction pressure (MPa), D is the relative density of the compact, and K and A are the constants. The tablet weight and thickness were recorded. The porosity, apparent density (g/cm^3), and relative densities of each compaction were calculated by Equations (11)–(13), respectively [25].

$$\text{Porosity } (\varepsilon) = 1 - D \tag{11}$$

$$\text{Apparent density } (\rho_A) = \frac{\text{Weight}}{\pi r^2 h} \tag{12}$$

$$\text{Relative density } (D) = \frac{\rho_A}{\rho_T} \tag{13}$$

where r, h and ρ_T are the tablet radius (cm), thickness (cm), and true density (g/cm^3) of the powder mixture, respectively. The true density of the powder mixture was measured by a pycnometer. The ln ($\frac{1}{1-D}$) was plotted against compaction pressure. The slope referred to the plasticity of the compressed substance. The reciprocal of the slope was the yield pressure of the substance, which was adversely related to the ability of the substance to deform plastically under the pressure. A lower value of yield pressure referred to easy compaction and greater plasticity.

2.3. Statistical analysis

For multiple comparisons across different groups, data are represented by the mean ± S.D. and were evaluated using one-way analysis of variance *(*ANOVA*)*, followed by Dunnett's Test. The statistical significance between two groups was ascertained using the student *t*-test. The significance of differences was set at $p < 0.05$.

3. Results and discussion

3.1. Preparation of cpGRS

It is challenging to improve the characteristics of a single excipient without compromising other functionalities because these properties could be in conflict with one another. For instance, improvements in compactibility may have an impact on the ability of disintegration. These issues are minimized with coprocessed excipients, which can achieve better multifunctional properties than individual ones. GRS's poor flowability and compactibility were overcome by the development of a coprocessed excipient that combined GRS, PVP K30, and calcium carbonate. CCD was the tool used to determine the proper amounts of sodium hydroxide solution, mixing time, pH at endpoint, amount of PVP K30, and calcium carbonate that would impart the highest percentage of yield and tensile strength with the lowest possible Carr's index, Hausner ratio, and disintegration time.

The starch granules were partially gelatinized and mildly swelled in 0.05 M sodium hydroxide solution to produce a white slurry. After adding the additive suspension, the starch granules were further gelatinized from the higher concentration of sodium hydroxide medium such that the starch slurry became thicker according to the content of the alkaline added. Hydrochloric acid was added later to the mixture to reverse the swelling of starch granules and induce the entrapment of calcium carbonate on the surface of the starch granules utilizing PVP K30 as a glue-like substance [13]. The precipitated products were filtered through a nylon sheet, washed with water, dried, and milled. cpGRS products appeared as white powder.

The characteristics of the cpGRS product were influenced by multiple factors, including the concentration of the alkaline solution,

the duration of mixing, the pH at endpoint, the type and quantity of added excipients. Increasing the concentration of the alkaline solution results in a higher degree of gelatinization and increased solubility in water. Moreover, the alkaline solution can dissolve certain portions of the starch surface granule, leading to the formation of surface voids that facilitate the incorporation of additives [26–29].

The solubility and molecular weight of starch are both influenced by the duration of mixing. As the mixing time increases, the structure of starch changes, leading to improved solubility. In the case of waxy corn starch, prolonged mixing initially results in an increase in molecular weight. However, after 20 min, the molecular weight decreases due to molecular breakdown [27]. The length of the amylopectin branch chain plays a critical role in determining the solubility, swelling capacity, and pasting abilities of starch granules [30].

The pH at the endpoint of the starch mixture can impact the length of the starch chain. Previous research has shown that starch molecules undergo complete degradation at non-neutral pH levels. Specifically, pH levels below 5 and above 10 result in starch molecules with a lower molecular mass compared to pH levels ranging from 7 to 9 [31].

The properties of modified starch are also influenced by the type and quantity of added excipients. For optimal performance, the additional excipients should exhibit either brittle or plastic deformation characteristics. In the case of GRS, which is a plastic deformed material [32–34], calcium carbonate, a material with brittle deformation properties, is selected. Calcium carbonate is commonly used as a tablet filler [17,18]. Furthermore, to enhance the adhesion of calcium carbonate to the starch surface, polyvinyl pyrrolidone K30 (PVP K30), a tablet binder exhibiting plastic deformation properties, is chosen.

The Design of Experiment (DoE) approach serves as an effective tool for optimizing multiple factors and obtaining desired responses. In this study, there are five factors of interest, comprising both process and formulation-related parameters. To achieve this, the central composite design (CCD) is chosen, as it combines the advantages of both factorial design and star design [35]. CCD involves a five-level experiment, retaining the main effect, quadratic term, and interaction. By utilizing this design, the experimental time and cost are significantly reduced compared to a full factorial design. CCD consists of a combination of factorial points (two-level full factorial points), axial points (varying only one component), and center points (all factors set at the midpoint) [36,37]. Compared to traditional methods such as orthogonal design and uniform design, CCD offers higher precision and the ability to identify optimal values across the entire range [38]. Utilizing a CCD with five levels, as opposed to three levels, provides more accurate modeling and optimization, greater flexibility for complex systems or nonlinear behavior, and robustness against experimental noise [35].

3.2. Physicochemical properties of cpGRS

3.2.1. The percentage yield, powder flowability and moisture content

Table 1 displays the physicochemical properties of cpGRS, GRS, calcium carbonate, and PVP K30. The yield of cpGRS was 68.8 ± 3.37%, with a bulk density of 0.57 ± 0.01 g/cm^3 and a tapped density of 0.69 ± 0.01 g/cm^3 cpGRS was denser than GRS and PVP K30 but less dense than calcium carbonate. The flow characteristics of cpGRS are demonstrated by the Carr's index and Hausner's ratio, which were 17.16 ± 1.07 and 1.21 ± 0.02, respectively. This was classified as fair to good flow characteristic, while native GRS had cohesive poor-flowing characteristic (Table 1). The results showed that cpGRS had improved flowability. This was due to the reduction of the interparticulate forces from increasing the roughness of the particle surface [13,39], and increasing the particle size (Fig. 3(c) and (d)). The cpGRS particle size was bigger than GRS with a volume weighted mean of 555.60 ± 16.93 μm.

The flowability of cpGRS in the current study showed improvement from poor to good, which is similar to a previous report examining rice starch-colloidal silicon dioxide coprecipitated powder [13]. In contrast, a chitosan-silicate coprecipitated powder showed improvement from poor to excellent flowability [40]. These variations in the degree of improvement may be attributed to differences in the coprecipitation process and composition. Nonetheless, the consistent trend observed in the data is that the coprecipitated approach consistently enhanced the powder's flow behavior across multiple investigations.

3.2.2. The molecular interaction and crystalline structure

The IR spectra of cpGRS, GRS, calcium carbonate, and PVP K30 are shown Fig. 1. Both cpGRS and GRS exhibit similar peak positions in the regions of 4000 to 2500 cm^{-1} and 800 to 400 cm^{-1}. The peaks at 3398 cm^{-1} and 2932 cm^{-1} correspond to the stretching vibrations of O–H and –CH_2 groups, respectively [41]. An additional peak observed in the range of 3398 to 2932 cm^{-1}, indicates a correlation with the level of hydration [42]. These peak intensities were found to be stronger in GRS compared to cpGRS, indicating a higher amount of moisture. This observation aligns with the higher moisture content measured in GRS compared to cpGRS (Table 1).

Table 1
Physicochemical properties of cpGRS, GRS, calcium carbonate, and PVP K30 (n = 3).

	cpGRS	GRS	Calcium carbonate	PVP K30
Bulk density (g/cm^3)	0.57 ± 0.01	0.33 ± 0.00[a]	0.80 ± 0.00[a]	0.34 ± 0.00[a]
Tapped density (g/cm^3)	0.69 ± 0.01	0.55 ± 0.01[a]	1.20 ± 0.00[a]	0.47 ± 0.00[a]
Carr's Index	17.16 ± 1.07	40.29 ± 0.34[a]	33.33 ± 0.00[a]	26.88 ± 0.00[a]
Hausner's Ratio	1.21 ± 0.02	1.67 ± 0.01[a]	1.50 ± 0.00[a]	1.37 ± 0.00[a]
Flowability	Fair to Good	Very poor	Very poor	Poor
Moisture content (%)	8.20 ± 0.14	11.80 ± 0.64[a]	0.44 ± 0.01[a]	17.67 ± 0.12[a]
Particle size (μm)	555.60 ± 16.93	15.32 ± 0.54[a]	10.95 ± 0.13[a]	96.96 ± 4.51[a]

[a] was statistically significant (p-value <0.05) in comparison to cpGRS.

Additionally, peaks at 764 cm^{-1}, 709 cm^{-1}, 576 cm^{-1}, and 530 cm^{-1} were identified as the skeletal mode vibrations of the pyranose ring in the glucose unit [41].

In the IR spectra of calcium carbonate, the prominent peaks corresponded to calcite, displaying peaks at 712 cm^{-1}, 873 cm^{-1}, and 1416 cm^{-1}. The peaks at 2980 cm^{-1} and 2873 cm^{-1} were attributed to the asymmetric and symmetric stretching vibrations of C–H bonds [43]. In the spectra of PVP K30, significant bands were observed at 2956 cm-1 and 1658 cm-1, corresponding to the stretching vibrations of C–H and C═O groups, respectively [44,45]. The spectra of cpGRS exhibited no noticeable variation or significant shift in these important peaks, suggesting the absence of any chemical interaction between GRS, calcium carbonate, and PVP K30, which was the main concept of co-processed excipient.

In order to describe the solid-state characteristics of the solid dispersion system, X-ray diffraction (XRD) analysis was carried out. This method is suitable for assessing how interactions affect the solid dispersion system's crystalline phase and amorphization [46]. Strong diffraction peaks were visible in the GRS XRD pattern at Bragg angles 2θ of 15.1°, 17.1°, 17.9°, and 23.2°, which is the typical A-type pattern of starch. Additionally, the cpGRS also demonstrated A-type pattern characteristics with peaks at Bragg angles (2θ) of 15.3°, 17.3°, 18.1°, and 23.1° (Fig. 2). PVP K-30's XRD pattern exhibited a broad and diffused pattern at Bragg angles of 12.0°and 21.1° due to the molecule's random arrangement inside the crystal lattice [47]. The calcium carbonate's peaks were seen at Bragg angles of 29.5°, 35.8°, 43.3°, 47.7°, 48.6°, etc. The XRD pattern coincided with the crystal phases of the calcium carbonate (calcite form) [48,49]. Both PM and cpGRS displayed diffraction peaks at the identical Bragg angles, indicating that both contained calcium carbonate. There was no peak loss and no new peaks in either PM or cpGRS, indicating that neither the crystallographic structure nor the lattice parameters had undergone any significant changes. Confirmation of the presence of GRS, calcium carbonate, and PVP K30 in the cpGRS was obtained by comparing the acquired XRD spectrum of cpGRS with those of GRS, calcium carbonate, and PVP K30. The XRD study ultimately confirmed that the cpGRS is composed of GRS, calcium carbonate, and PVP K30. Previous reports using XRD analysis of chitin and metal silicates coprecipitation [50] and rice starch and colloidal silicon dioxide coprecipitation [13] also showed no significant changes in their XRD spectra.

3.2.3. The surface morphology and particle size distribution

The surface morphology and microstructure of the cpGRS, GRS, calcium carbonate (Fig. 3 (b)), and PVP K30 (Fig. 3 (a)) were visually revealed by the SEM investigation. The SEM images in Fig. 3(c) and (e) illustrate that GRS has a polygonal shape [2,51], is non-porous, and has a smooth surface. Fig. 3(d) and (f) show calcium carbonate particles that were co-precipitated onto the surface of starch granules after modification. This made the surface of the starch particles rougher. Both large and small particle sizes were visible in the cpGRS.

A previous study on rice starch and colloidal silicon dioxide co-precipitation also demonstrated the deposition of colloidal silicon dioxide on the surface of rice starch granules [13]. Similarly, the surfaces of maize starch were coated with magnesium silicate [14]. These findings provide evidence that the precipitating of excipients onto the surface of modified starch granules results in a rougher surface of the starch particles.

In this study, the crystalline structure of cpGRS was validated by XRD analysis, and SEM was employed to analyze the microstructure. The composition of the cpGRS was deduced through the identification of distinctive peaks in the XRD spectrum. The GRS, calcium carbonate, and PVP K30 peaks were compared to the cpGRS XRD peaks. Peak locations were compared in order to determine the crystalline structure of cpGRS. The combined SEM and XRD analysis provided trustworthy validation of the cpGRS's composition and crystalline structure without relying on elemental mapping, even if energy-dispersive X-ray (EDX) spectroscopy was not performed in this case.

3.3. cpGRS tablets properties

The cpGRS tablets, without drugs and lubricant, had a tensile strength of 3.05 ± 0.29 MPa and a disintegration time of 224.05 ±

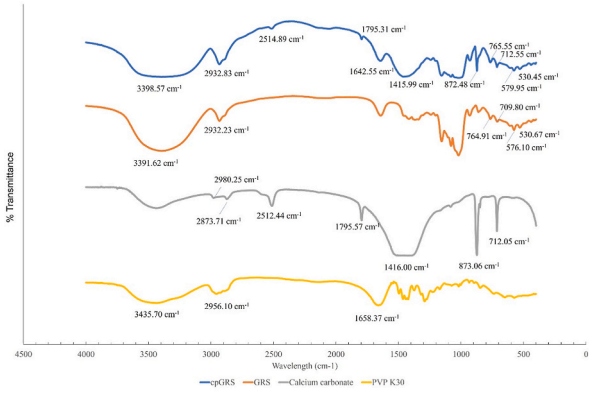

Fig. 1. The FT-IR spectra of cpGRS, GRS, calcium carbonate, and PVP K30.

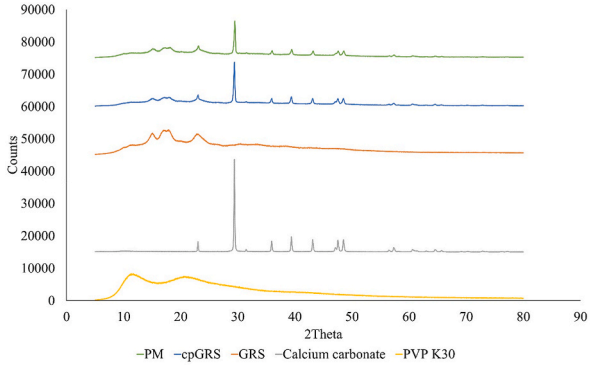

Fig. 2. Powder X-ray diffractograms of PM, cpGRS, GRS, calcium carbonate, and PVP K30.

25.10 secounds. The tensile strength of cpGRS tablets (3.05 ± 0.29 MPa) was a little bit lower than that of GRS tablets (3.87 ± 0.13 MPa), while their disintegration times were comparable (224.05 ± 25.10 vs 217.67 ± 3.61 s, respectively). Although the cpGRS preparations had a lower tensile strength than GRS, they nonetheless retained a tensile strength that was acceptable for tablet manufacturing.

When compared to previous reports, the tablet strength of cpGRS was found to be higher than that of co-precipitated rice starch and colloidal silicon dioxide [13], but lower than that of co-precipitated starch and magnesium silicate [14]. These differences could be attributed to variations in tablet composition, compression force, or tablet size used in different trials.

This study showed that the disintegration times of cpGRS and GRS were similar, with both completed in 4 min, which was shorter than the suggested disintegration time for immediate release tablets (within 15 min). This qualified them as potential candidates for use in formulations for immediate release tablets. When comparing the results of cpGRS with several earlier studies, minor variations in disintegration time values were observed. The disintegration time of cpGRS (4 min) was longer than that of coprecipitated chitosan-silica (5 s) [40], starch-magnesium silicate (<1 min) [14] and chitin-metal silicate (<1 min) [52]. However, all of these disintegration times remain remarkably short.

3.4. Dilution potential

Dilution potential is an important parameter of excipients for direct compression tablet preparation. It is used to determine the amount of drug that can be incorporated into tablets while keeping desirable mechanical properties with respect to hardness and friability [53]. Paracetamol was used as a model drug because of its poor compaction property and elastic recovery after removal of the compaction pressure [54]. Commonly, the mechanical strength of the compact increased as the ratio of the excipients relative to the drug increased. The dilution potential plot illustrated the relationship between the % paracetamol content and the tensile strength of the tablet at different compaction pressures (Fig. 4). Normalizing the AUC of each mixture of paracetamol/cpGRS by dividing the AUC of each mixture by the AUC of a 0% w/w mixture gave the ratio known as work potential or area ratio. This area ratio was plotted against the % w/w of paracetamol to cpGRS. The linear regression, which was extrapolated to zero area ratio, exhibited the value of the dilution capacity [20]. In this study, the cpGRS had dilution capacity value of 50% w/w paracetamol (Fig. 5), which indicates that cpGRS can hold a maximum of 50% w/w paracetamol while maintaining desirable hardness and friability.

cpGRS demonstrated a dilution capacity superior to the 30–40% by weight range of the majority of directly compressible excipients [55]. This excipient proved to be beneficial for direct compression, even with paracetamol, which is known for its difficult compressibility.

3.5. Lubricant sensitivity

Lubricant is commonly used for reducing die wall friction during tablet compaction and ejection. The effect of lubricant on a tablet's hardness depends on factors such as the nature and concentration of the lubricant and the mixing time. In addition, the deformation of material also affects lubricant sensitivity [56]. Lubricant sensitivity is expressed in terms of LSR, which represents the decrease in tablet hardness with and without lubricant [21]. Dry powder is increasingly susceptible to additional lubricant as the LSR value gets closer to 1 [57]. Magnesium stearate is the most commonly used pharmaceutical lubricant, with typical concentrations ranging from 0.25 to 5%. It has been demonstrated that magnesium stearate can negatively affect the bonding between particles, which reduces the strength of tablets [18,58,59].

Fig. 6(a) shows the lubricant sensitivity of four excipients. All tablet tensile strengths were reduced by lubricant, especially PGS, which could not compact into tablets when magnesium stearate content was more than 1% w/w. The LSR values for the excipients at 5% w/w of magnesium stearate content were ranked PGS > cpGRS > CS90 > PM, (Fig. 6(b)). The tensile strength of cpGRS tablets decreased by more than PM and CS90 as the amount of lubricant rose suggesting that cpGRS was more susceptible to the lubricant than

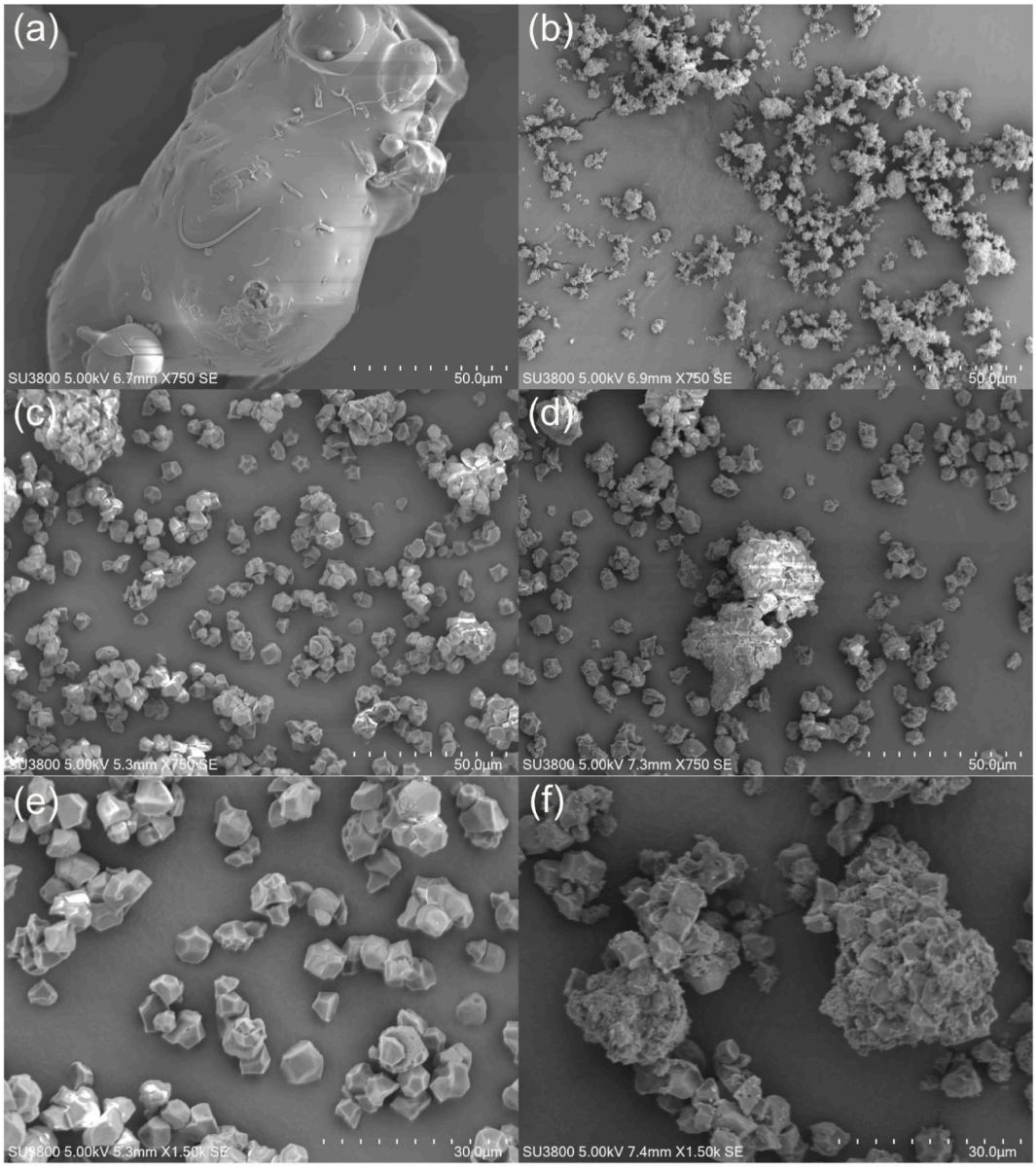

Fig. 3. The SEM images of: (a) PVP K30 at a magnification of ×750; (b) calcium carbonate at a magnification of ×750; (c) GRS at a magnification of ×750; (d) cpGRS at a magnification of ×750; (e) GRS at a magnification of ×1500; and (f) cpGRS at a magnification of ×1500.

PM and CS90. However, cpGRS tablets still demonstrated a stronger tensile strength than CS90 (2.52 ± 0.09, 2.19 ± 0.10, respectively) even at 5% of magnesium stearate in tablets, while PGS was unable to compact into tablets. This could be because the more plastic cpGRS has a higher lubricant sensitivity than the more brittle CS90 [56]. The tensile strengths of cpGRS compacts were weaker than PM at 0.5% w/w of magnesium stearate content and this may be a result of the impact of the particle size. According to a prior study, smaller particles are less susceptible to lubricants than bigger particles, which leads to a smaller LSR. The percentage of the surface covered by lubricant is lower for a powder with a smaller particle size incorporating the same amount of lubricant and using the same mixing time. For larger particles, the lubricant covers a larger portion of the accessible bonding space. This causes the effect of the initial particle size on compact strength to be worse with added lubricant than it would be without lubricant [56]. In order to ensure that a tablet is mechanically strong enough to endure commercial manufacturing and subsequent transportation, a tensile strength of at least 1.7 MPa is generally adequate. For small batches of tablets that are not subjected to high mechanical stresses, tensile strengths as low as 1 MPa may be sufficient [60,61]. Thus, even with the highest percentage of magnesium stearate in the tablets, the cpGRS preparations retained a tensile strength greater than 1.7 MPa, which is a suitable tensile strength for tablet manufacture.

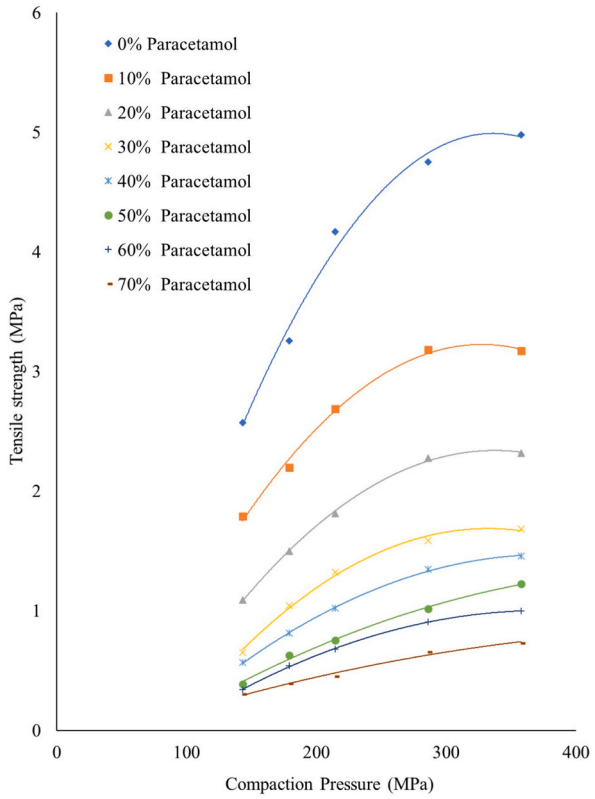

Fig. 4. The dilution potential plot of cpGRS.

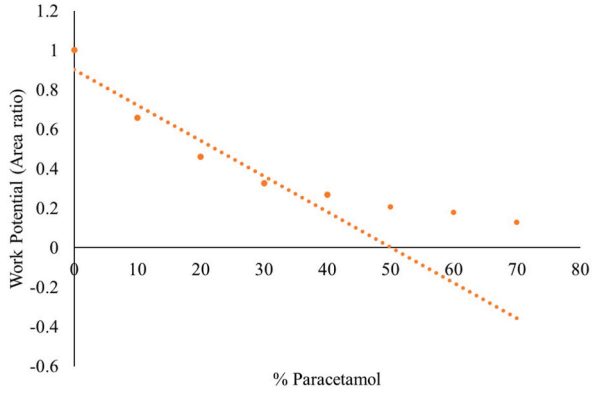

Fig. 5. The work potential plot of cpGRS.

3.6. The medicated tablet production

The objective of this study was to examine how the solubility of an API can affect the pharmaceutical properties of cpGRS. The model drugs used to prepare the medicated tablets were domperidone and propranolol hydrochloride, which are classified as class I and II, respectively, in the Biopharmaceutics Classification System (BCS). Class I category drugs have high solubility and permeability and were chosen for testing because of their consistently high fraction of absorption, regardless of formulation [62,63]. BCS class II APIs have low solubility and high permeability so the barrier to their absorption is dissolution, which is dependent on the API's solubility. The solubility of an API affects how it dissolves from a dosage form. Approximately 40% of the newest APIs have poor water solubility, and their main drawback is a slower rate of dissolution in the compact solid dosage form. To increase the low dissolution rate of water-insoluble drugs, a number of techniques have been used, including size reduction, complexation, and microencapsulation. However, using the right formulation excipients also makes it possible to increase API solubility [64].

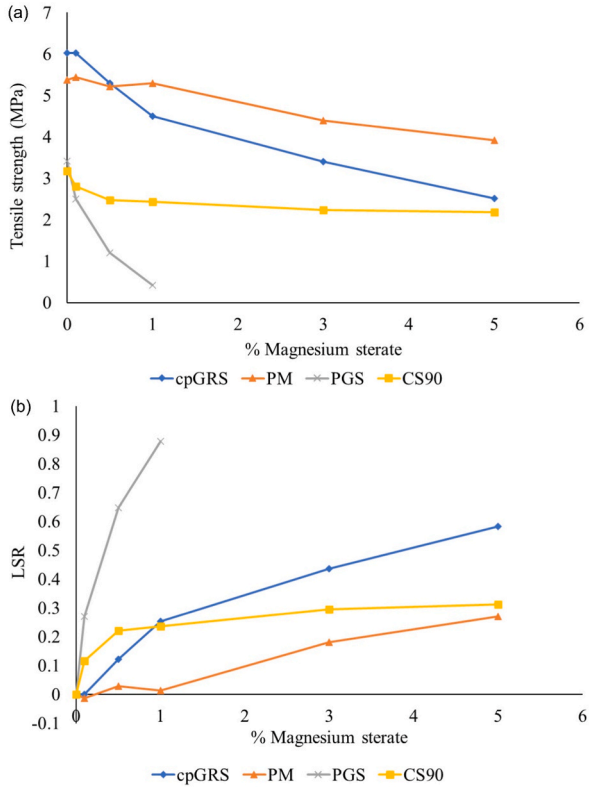

Fig. 6. Lubricant sensitivity plots: (a) Tensile strength of four excipients with different concentration of magnesium stearate; (b) LSR of four excipients with different concentration of magnesium stearate.

The ratios of API to excipient used in the formulations should be those given by the dilution potential value (50%). However, PGS was unable to be compacted into tablets with a 50% propanolol content. As a result, the drug content was decreased to 30% to prepare propranolol and domperidone tablets with all excipients i.e., cpGRS, PM, PGS, and CS90.

3.7. Pharmaceutical properties of the medicated tablets

3.7.1. Compactibility of cpGRS

The hardness of the tablets compacted at various compaction pressures was used to evaluate the tablets' compactibility. Fig. 7 illustrates how the compaction pressure significantly affected the mechanical strength of all medicated tablets. The findings demonstrated that, tablet hardness grew as compaction pressure increased until a particular pressure was achieved, at that point a higher compaction pressure caused a fall in the slope of the line of hardness [65]. Compactibility of cpGRSs, PM, PGS, and CS90 are compared as the slope of the PHP (Fig. 7). Propanolol-cpGRS compacts displayed a higher PHP slope than PGS and CS90, but lower than PM tablets (Fig. 7 (a) and **Supplementary file 2**), demonstrating that cpGRS is easier to compress compared to PGS and CS90. For domperidone, cpGRS compacts demonstrated a higher PHP slope than PM, PGS, and CS90 (Fig. 7 (b) and **Supplementary file 2**), demonstrating that cpGRS was the easiest to compress.

The ability of the powder to be compressed into tablets, which imparts the tablet shape, and porosity, is determined by the compaction properties of tablet. There are numerous mathematical models that can be used to investigate mechanical aspects of the compaction properties of powder. The Heckel analysis is the most frequently used model to describe these aspects. The Heckel coefficient, also known as the mean yield pressure, is an indicator of a material's capacity for plastic deformation. It is calculated using the slope of the linear part of the Heckel plot (Fig. 8). The yield pressure is given by the inverse value of the slope (K) from the Heckel plot. Materials that have a more plastic character are thought to have lower yield pressure. High yield pressure values demonstrate the high resistance to compaction and volume reduction. Low yield pressure suggests that plastic deformation during compression starts more quickly. In general, a low yield pressure value indicates good densification, easy compression, and low pressure resistance [25].

In both propranolol and domperidone tablets, the yield value for cpGRS was found to be the lowest (303.03 and 270.27 respectively), indicating that it has better deforming capacity than PM, PGS, and CS90 (**Supplementary file 2** and Fig. 8 (a) and (b)). This may have been caused by the impact of the mechanical characteristics of the other components on the dominant plasticity of starch. Thus, when PVP K30, as a plastic material, and calcium carbonate, as a brittle material, were co-precipitated with starch to create a single composite excipient, this resulted in starch with brittle elements, which in turn caused cpGRS to have a better yield pressure.

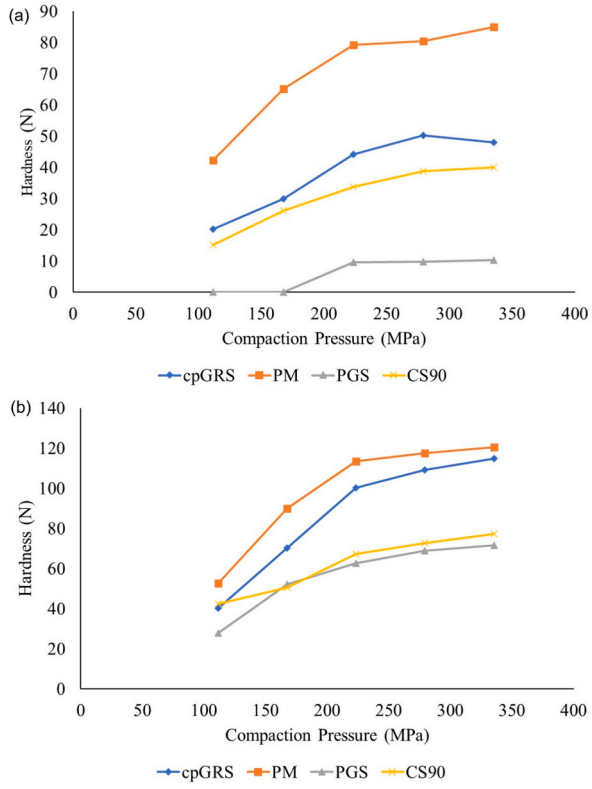

Fig. 7. PHP of cpGRS, PM, PGS, and CS90: (a) propranolol; and (b) domperidone tablets.

Therefore, co-precipitating improved the compactibility of cpGRS. Calcium carbonate may have enhanced the particle structure's bonding strength per unit area, resulting in compacts with rising tensile strength. Additionally, the presence of calcium carbonate enhances brittleness, which causes particles to fracture when compressed and create new contact surfaces that are more prominent than in plastic deformation [66].

3.7.2. The tablet hardness

Hardness is an empirical attribute that is a convenient and helpful measurement for in-process control and quality assurance. Tensile strength is a characteristic of compressed material and is a fundamental parameter that preserves consistency even when the size of the tablet is altered [67]. The hardness of cpGRS, PM, PGS, and CS90 propranolol tablets are displayed in Fig. 9(a). The ranking of hardness of propranolol tablets made with various excipients was PM > cpGRS = CS90 > PGS tablets (Fig. 9). But when the dimension of the tablets was included in the consideration, the tensile strength of CS90-propranolol tablet was a little bit higher than cpGSR tablets. However, both cpGRS hardness and tensile strength were still high enough for general use in daily life [61,68].

The hardness and tensile strengths of domperidone tablets were higher than propranolol tablets for all excipient types. The hardness were ranked PM > cpGRS > PGS = CS90 and the tensile strengths were ranked PM > cpGRS > CS90 > PGS. The PGS tablets had comparable hardness to CS90, but lower tensile strength. This occurred because PGS tablets were thicker than CS90 tablets. PGS particles may have recovered their original shapes after undergoing elastic deformation, which made the PGS tablets thicker than CS90 tablets [16,69]. The cpGRS could make tablets with a high hardness and tensile strength [61,68].

In both medicated tablets, the order of hardness and tensile strength were a little bit different. This is because the thickness of the tablets was different due to the compactibility properties of each excipient. In comparison to both model drugs, the hardness and tensile strengths of PM tablets were the highest and PGS tablets were the lowest. This might be explained by PVP K30's binding properties [18], which might be present in higher concentrations in the PM than the cpGRS. The cpGRS may lose some PVP K30 during the washing steps of preparation. PGS can be compressed easily, however compacts had poor strength. This was due to the fact that elastic deformation made up a large portion of the final deformation and that in the case of fast compression, plastic deformation was too slow to establish sufficient interparticular connections [69]. As a result, cpGRS that had undergone partial pregelatinization displayed less tensile strength and hardness than PM. This might be because the cpGRS pregelatinization region exhibits elastic deformation capabilities.

3.7.3. Friability

The test for tablet friability determines how well tablets can endure stresses from handling and shipping. Tablets should exhibit a

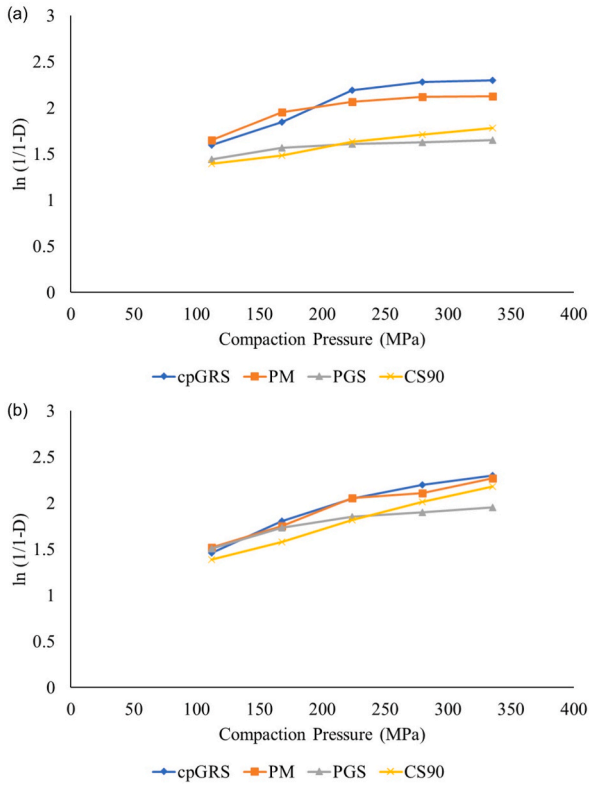

Fig. 8. Heckel plots of cpGRS, PM, PGS, and CS90: (a) propranolol; and (b) domperidone.

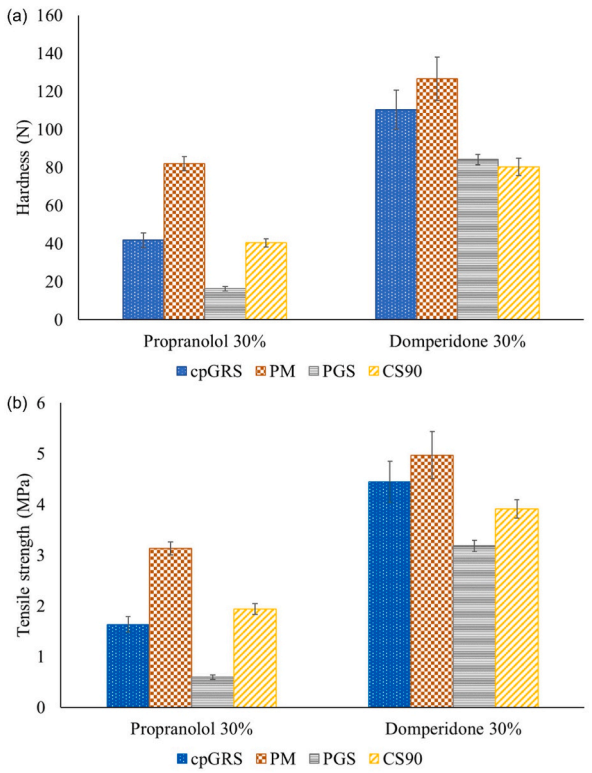

Fig. 9. Tablet strength plots of propranolol and domperidone: (a) hardness; and (b) tensile strength of cpGRS, PM, PGS, and CS90.

weight loss of no more than 1%, in accordance with USP44/NF39 [22]. Fig. 10 provides a summary of the tablet friability test performed on medicated tablets made by cpGRS, PM, PGS, and CS90. With the exception of the formulation containing PGS-propranolol, all formulations passed the friability test. The plastic-elastic nature of PGS may be the cause of the PGS-propranolol tablets' weakness. PGS possessed a low degree of plasticity (**Supplementary file 2**), which accounted for its poor binding capacity and low tensile strength. Moreover, elastic recovery contributed to the final deformation, increasing the PGS tablet friability [69].

3.7.4. Disintegration times

The disintegration time of tablets containing model drugs i.e., propranolol and domperidone and excipients i.e., cpGRS, PM, PGS, and CS90 was investigated and is shown in Fig. 11. For an immediate release tablet, 15 min is the recommended time for full breakdown. All propranolol tablets disintegrated faster than 15 min (Fig. 11). For domperidone tablets, only cpGRS and PM met the criteria. The ranking of the disintegration times for the propranolol tablets were cpGRS = CS90 < PM < PGS. The cpGRS and CS90 disintegration times were 1.4 and 2.5 times faster than the PM and PGS formulations, respectively. The order of the disintegration times for domperidone tablets was cpGRS < PM < CS90 < PGS. The best disintegration property was demonstrated by cpGRS, which disintegrated 2, 52.6, and 72.6 times faster than PM, CS90, and PGS formulations, respectively.

PGS combined characteristics of native and completely gelatinized starches. A significant portion of disintegration properties were lost due to gelatinization. Because of this, they had longer disintegration times than cpGRS and PM. However, the PVP K30 is a binder [18], and it is possible that it was present in the PM in larger amounts than it was in the cpGRS. This could explain why the cpGRS had shorter disintegration times than the PM. As a result, cpGRS is an excellent candidate to be used in a formulation for disintegrating immediate release tablets.

3.7.5. Dissolution tests

The dissolution test was carried out at 37 ± 0.5 °C in three different mediums: 0.1 N HCl (pH 1.2) to simulate gastric fluid without enzyme, acetate buffer (pH 4.5), and phosphate buffer (pH 6.8) to mimic intestinal fluid without enzyme. With the exception of propranolol-CS90 in pH 6.8 medium (**Supplementary file 3**), the other propranolol dissolution profiles demonstrated cumulative drug release of more than 80% after 10 min, which met the USP criteria in all media (**Supplementary file 3**) [22]. The dissolution studies in pH 1.2, 4.5 and 6.8 mediums were conducted to characterize the behavior of cpGRS across the entire gastrointestinal tract. The outcome demonstrated that the drug release profile of the propranolol-cpGRS formulation was not affected by the pH of dissolution medium (Fig. 12). The cpGRS produced fastest and highest drug release than other excipients in all medium.

In contrast, the dissolution profile of all domperidone tablets in pH 6.8 did not meet the USP criteria (**Supplementary file 3**). It was observed that there were differences in the disintegration pattern for each excipient with domperidone tablets. cpGRS, PM, and PGS domperidone tablets disintegrated into small pieces, but CS90 domperidone tablets disintegrated into big flakes. The release rate of domperidone tablets in pH 1.2 medium was higher than in pH 4.5, and pH 6.8 medium, respectively. This result is concordant with the solubility profile of domperidone in different pH medium [23,70]. The lower the pH of the medium, the higher the solubility of domperidone. The domperidone release profile was influenced by the pH of the dissolution medium (Fig. 13). Therefore, care should be taken when using cpGRS with an insoluble API.

4. Conclusions

The cpGRS was optimally prepared at 0.43 M of sodium hydroxide solution, 7.09% of PVP K30, 14.02% of calcium carbonate, and 95 min of mixing time with an end pH of 6.97. This resulted in the yield of 68.8 ± 3.37%, flowability with Carr's index of 17.16 ± 1.07, and Hausner ratio of 1.21 ± 0.02. The cpGRS tablets had a tensile strength of 3.05 ± 0.29 MPa and disintegration time of 3 min 44 s ± 25.1 s. There were no chemical interactions between ingredients. cpGRS showed a considerable improvement in physicochemical properties, i.e., higher density and better flowability. It had 50% dilution potential when using paracetamol as a model drug. The cpGRS was slightly sensitive to lubricant (magnesium stearate), however the hardness and tensile strengths were a lot higher than common strength for general purpose use of tablets. Compactibility of cpGRS with both propranolol and domperidone was improved. This process could produce tablets with high hardness and tensile strength, low friability, and fast disintegration. For propranolol-cpGRS tablets, dissolution medium at different pH did not affect the dissolution profile. For domperidone-cpGRS tablets, the pH of dissolution medium affected the dissolution profile of the tablets, which was according to domperidone's solubility and could cause some concern with using APIs that are not soluble. The study's findings demonstrated that cpGRS is an excellent multifunctional i.e., filler, binder, and disintegrant direct compression excipient candidate. The main component is natural, the preparation method was simple, requires only basic equipment, uses affordable reactants, quick, and efficient and does not produce harmful waste.

Funding

This research was partially funded by Faculty of Pharmaceutical Sciences, Khon Kaen University, Thailand.

Author contribution statement

Chonticha Amornrojvaravut: onceived and designed the experiments; Performed the experiments; Analyzed and interpreted the data; Wrote the paper.

Jomjai Peerapattana: onceived and designed the experiments; Analyzed and interpreted the data; Contributed reagents, materials,

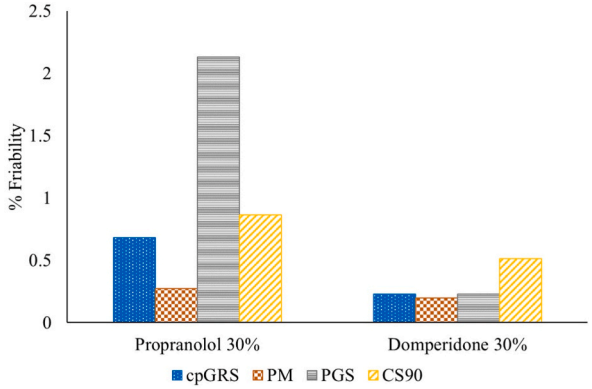

Fig. 10. Propranolol and domperidone tablet friability plots in the cpGRS, PM, PGS, and CS90.

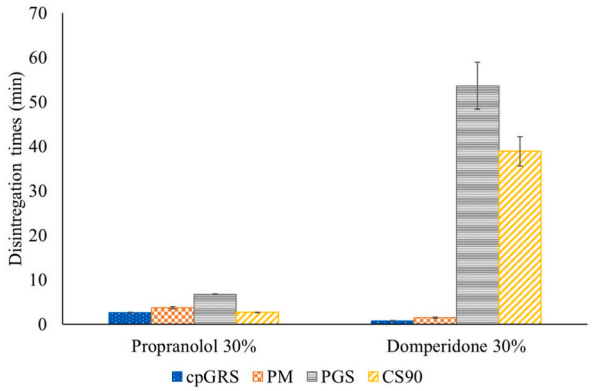

Fig. 11. Propranolol and domperidone disintegration times plots in the cpGRS, PM, PGS, and CS90.

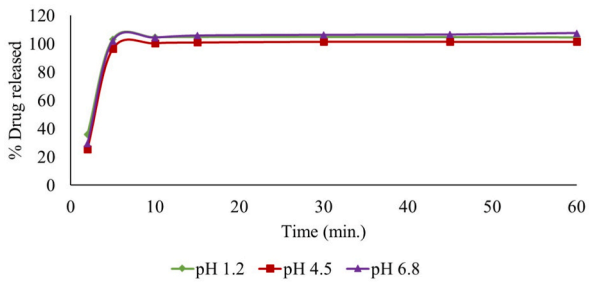

Fig. 12. Compiled release profiles of propranolol-cpGRS formulation in three different pH media.

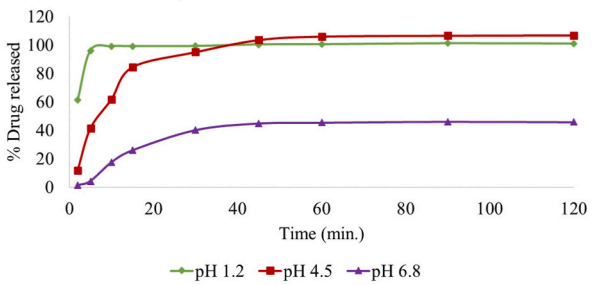

Fig. 13. Compiled release profiles of domperidone-cpGRS formulation in three different pH media.

analysis tools or data; Wrote the paper.

Data availability statement

Data will be made available on request.

Declaration of competing interest

The authors declare that they have no known competing financial interests or personal relationships that could have appeared to influence the work reported in this paper.

Acknowledgments

We would like to acknowledge Dr. Glenn Neville Borlace, for editing the MS via Publication Clinic KKU, Thailand.

Appendix A. Supplementary data

Supplementary data to this article can be found online at https://doi.org/10.1016/j.heliyon.2023.e19904.

References

[1] G.K. Bolhuis, N.A. Armstrong, Excipients for direct compaction–an update, Pharmaceut. Dev. Technol. 11 (2006) 111–124.
[2] P. Laovachirasuwan, J. Peerapattana, V. Srijesdaruk, P. Chitropas, M. Otsuka, The physicochemical properties of a spray dried glutinous rice starch biopolymer, Colloids Surf. B Biointerfaces 78 (2010) 30–35.
[3] L. Pachuau, R.S. Dutta, P.K. Roy, P. Kalita, H. Lalhlenmawia, Physicochemical and disintegrant properties of glutinous rice starch of Mizoram, India, Int. J. Biol. Macromol. 95 (2017) 1298–1304.
[4] E. Lahdenpaeae, M. Niskanen, J.K. Yliruusi, Crushing strength, disintegration time and weight variation of tablets compressed from three Avicel® PH grades and their mixtures, Eur. J. Pharm. Biopharm. 43 (1997) 315–322.
[5] M.V. Lawal, M.A. Odeniyi, O.A. Itiola, Effect of thermal and chemical modifications on the mechanical and release properties of paracetamol tablet formulations containing corn, cassava and sweet potato starches as filler-binders, Asian Pac. J. Trop. Biomed. 5 (2015) 585–590.
[6] A. Mondal, K.J. Kumar, Effect of thermal modification on the release characteristics of pink potato starch of Jharkhand, India, Int. J. Biol. Macromol. 140 (2019) 1091–1097.
[7] M.V. Lawal, M.A. Odeniyi, O.A. Itiola, Material and rheological properties of native, acetylated, and pregelatinized forms of corn, cassava, and sweet potato starches, Starch - Stärke 67 (2015) 964–975.
[8] K. Hauschild, K.M. Picker, Evaluation of a new coprocessed compound based on lactose and maize starch for tablet formulation, AAPS J. 6 (2004) 27–38.
[9] P.F. Builders, A.M. Bonaventure, A. Tiwalade, L.C. Okpako, A.A. Attama, Novel multifunctional pharmaceutical excipients derived from microcrystalline cellulose-starch microparticulate composites prepared by compatibilized reactive polymer blending, Int. J. Pharm. 388 (2010) 159–167.
[10] A. Olowosulu, A. Oyi, A. Isah, M. Ibrahim, Formulation and evaluation of novel coprocessed excipients of maize starch and Acacia gum (StarAc) for direct compression tabletting, Int. J. Pharmaceut. Res. Innovat. 2 (2011).
[11] D. Kankate, S.G. Panpalia, K.J. Kumar, J.F. Kennedy, Studies to predict the effect of pregelatinization on excipient property of maize and potato starch blends, Int. J. Biol. Macromol. 164 (2020) 1206–1214.
[12] V. Limwong, N. Sutanthavibul, P. Kulvanich, Spherical composite particles of rice starch and microcrystalline cellulose: a new coprocessed excipient for direct compression, AAPS PharmSciTech 5 (2004) e30-e30.
[13] O.S. Kittipongpatana, N. Kittipongpatana, Preparation and physicomechanical properties of co-precipitated rice starch-colloidal silicon dioxide, Powder Technol. 217 (2012) 377–382.
[14] I. Rashid, M. Al-Remawi, S.A. Leharne, B.Z. Chowdhry, A. Badwan, A novel multifunctional pharmaceutical excipient: modification of the permeability of starch by processing with magnesium silicate, Int. J. Pharm. 411 (2011) 18–26.
[15] S. Jain, Mechanical properties of powders for compaction and tableting: an overview, Pharmaceut. Sci. Technol. Today 2 (1999) 20–31.
[16] S. Mohan, Compression physics of pharmaceutical powders: a review, Int. J. Pharmaceut. Sci. Res. 3 (2012) 1580.
[17] S. Saha, A.F. Shahiwala, Multifunctional coprocessed excipients for improved tabletting performance, Expet Opin. Drug Deliv. 6 (2009) 197–208.
[18] R.C. Rowe, P.J. Sheskey, M.E. Quinn, Handbook of Pharmaceutical Excipients, Pharmaceutical Press, Greyslake, IL : Washington, DC, 2009.
[19] J. Peerapattana, P. Phuvarit, V. Srijesdaruk, D. Preechagoon, A. Tattawasart, Pregelatinized glutinous rice starch as a sustained release agent for tablet preparations, Carbohydr. Polym. 80 (2010) 453–459.
[20] Y. Habib, L. Augsburger, G. Reier, T. Wheatley, R. Shangraw, Dilution potential: a new perspective, Pharmaceut. Dev. Technol. 1 (1996) 205–212.
[21] C.E. Bos, H. Vromans, C.F. Lerk, Lubricant sensitivity in relation to bulk density for granulations based on starch or cellulose, Int. J. Pharm. 67 (1991) 39–49.
[22] C. United, States Pharmacopeial, the United States Pharmacopeia 44: the National Formula 39, United States Pharmacopeial Convention, Rockville, MD, 2021.
[23] E.A. Ahmed, I.A.-R. Sayed, O.A. Mahrous, A.Y. Mahmoud, Improvement of domperidone solubility and dissolution rate by dispersion in various hydrophilic carriers, J. Appl. Pharmaceut. Sci. 6 (2016) 133–139.
[24] O. Anand, L.X. Yu, D.P. Conner, B.M. Davit, Dissolution testing for generic drugs: an FDA perspective, AAPS J. 13 (2011) 328–335.
[25] J.M. Sonnergaard, A critical evaluation of the Heckel equation, Int. J. Pharm. 193 (1999) 63–71.
[26] T. Nagamine, K. Komae, Improvement of a method for chain-length distribution analysis of wheat amylopectin, J. Chromatogr. A 732 (1996) 255–259.
[27] J.-A. Han, S.-T. Lim, Structural changes in corn starches during alkaline dissolution by vortexing, Carbohydr. Polym. 55 (2004) 193–199.
[28] G.G. Maher, Alkali gelatinization of starches, Starch - Stärke 35 (1983) 226–234.
[29] A.J. Palacios-Fonseca, J. Castro-Rosas, C.A. Gómez-Aldapa, T. Tovar-Benítez, B.M. Millán-Malo, A. del Real, M.E. Rodríguez-García, Effect of the alkaline and acid treatments on the physicochemical properties of corn starch, CyTA - J. Food 11 (2013) 67–74.
[30] S.C. Alcázar-Alay, M.A.A. Meireles, Physicochemical properties, modifications and applications of starches from different botanical sources, Food Sci. Technol. 35 (2015) 215–236.
[31] J.H. Lee, J.-A. Han, S.-T. Lim, Effect of pH on aqueous structure of maize starches analyzed by HPSEC-MALLS-RI system, Food Hydrocolloids 23 (2009) 1935–1939.

[32] I. Ilić, B. Govedarica, R. Šibanc, R. Dreu, S. Srčič, Deformation properties of pharmaceutical excipients determined using an in-die and out-die method, Int. J. Pharm. 446 (2013) 6–15.
[33] X.H. Li, L.J. Zhao, K.P. Ruan, Y. Feng, D.S. Xu, K.F. Ruan, The application of factor analysis to evaluate deforming behaviors of directly compressed powders, Powder Technol. 247 (2013) 47–54.
[34] O.A. Odeku, O.A. Itiola, Compaction properties of three types of starch, Iran. J. Pharm. Res. (IJPR) 6 (2010) 17–23.
[35] B. Singh, R. Kumar, N. Ahuja, Optimizing drug delivery systems using systematic "design of experiments." Part I: fundamental aspects, Crit. Rev. Ther. Drug Carrier Syst. 22 (2005) 27–105.
[36] P. Sahoo, T.K. Barman, 5 - ANN modelling of fractal dimension in machining, in: J.P. Davim (Ed.), Mechatronics and Manufacturing Engineering, Woodhead Publishing, 2012, pp. 159–226.
[37] B. Wu, Chapter 2 - technical background, in: B. Wu (Ed.), Reliability Analysis of Dynamic Systems, Academic Press, Oxford, 2013, pp. 25–41.
[38] J. Li, X. Lin, F. Wu, L. Shen, Y. Wang, Y. Feng, Application of the central composite design to optimize the calcium carbonate-HPMC co-processed excipient prepared by co-spray drying, RSC Adv. 5 (2015) 94105–94114.
[39] Q. Zhou, B. Armstrong, I. Larson, P.J. Stewart, D.A. Morton, Improving powder flow properties of a cohesive lactose monohydrate powder by intensive mechanical dry coating, J. Pharmaceut. Sci. 99 (2010) 969–981.
[40] M. El-Barghouthi, A. Eftaiha, I. Rashid, M. Al-Remawi, A. Badwan, A novel superdisintegrating agent made from physically modified chitosan with silicon dioxide, Drug Dev. Ind. Pharm. 34 (2008) 373–383.
[41] R. Kizil, J. Irudayaraj, K. Seetharaman, Characterization of irradiated starches by using FT-Raman and FTIR spectroscopy, J. Agric. Food Chem. 50 (2002) 3912–3918.
[42] F.J. Warren, M.J. Gidley, B.M. Flanagan, Infrared spectroscopy as a tool to characterise starch ordered structure—a joint FTIR–ATR, NMR, XRD and DSC study, Carbohydr. Polym. 139 (2016) 35–42.
[43] C. Matei, D. Berger, A. Dumbrava, M.D. Radu, E. Gheorghe, Calcium carbonate as silver carrier in composite materials obtained in green seaweed extract with topical applications, J. Sol. Gel Sci. Technol. 93 (2020) 315–323.
[44] O.A. Sammour, M.A. Hammad, N.A. Megrab, A.S. Zidan, Formulation and optimization of mouth dissolve tablets containing rofecoxib solid dispersion, AAPS PharmSciTech 7 (2006). E55-E55.
[45] G.M. El Maghraby, R.N. Elsergany, Fast disintegrating tablets of nisoldipine for intra-oral administration, Pharmaceut. Dev. Technol. 19 (2014) 641–650.
[46] M.C. Adeyeye, 2 drug-excipient interaction occurrences during solid dosage form development, in: M.C. Adeyeye, H.G. Brittain (Eds.), Preformulation in Solid Dosage Form Development, CRC Press, Boca Raton, 2008, p. 80.
[47] P.S. Yadav, V. Kumar, U.P. Singh, H.R. Bhat, B. Mazumder, Physicochemical characterization and in vitro dissolution studies of solid dispersions of ketoprofen with PVP K30 and d-mannitol, Saudi Pharmaceut. J. 21 (2013) 77–84.
[48] R. Ranjan, S.D. Narnaware, N.V. Patil, A novel technique for synthesis of calcium carbonate nanoparticles, Natl. Acad. Sci. Lett. 41 (2018) 403–406.
[49] C.G. Kontoyannis, N.V. Vagenas, Calcium carbonate phase analysis using XRD and FT-Raman spectroscopy, Analyst 125 (2000) 251–255.
[50] I. Rashid, N. Daraghmeh, M. Al-Remawi, S.A. Leharne, B.Z. Chowdhry, A. Badwan, Characterization of chitin-metal silicates as binding superdisintegrants, J. Pharmaceut. Sci. 98 (2009) 4887–4901.
[51] W. Tharanon, J. Peerapattana, The effects of ball mill processing on the physicochemical properties of glutinous rice starch, Thai Journal of Pharmaceutical Sciences 44 (2020) 91–98.
[52] R.A.-S. Hamid, F. Al-Akayleh, M. Shubair, I. Rashid, M.A. Remawi, A. Badwan, Evaluation of three chitin metal silicate co-precipitates as a potential multifunctional single excipient in tablet formulations, Mar. Drugs 8 (2010) 1699–1715.
[53] O. Adeoye, G. Alebiowu, Flow, packing and compaction properties of novel coprocessed multifunctional directly compressible excipients prepared from tapioca starch and mannitol, Pharmaceut. Dev. Technol. 19 (2014) 901–910.
[54] G. Alderborn, C. Nyström, Radial and axial tensile strength and strength variability of paracetamol tablets, Acta Pharm. Suec. 21 (1984) 1–8.
[55] G.M. Khalid, H. Musa, A. Olowosulu, I. Jatau Abubakar, S. Ilyasu, M. Gwarzo, Comparative FTIR, compaction and in vitro dissolution studies of plectranthus esculentus modified starches in metronidazole tablet formulations by direct compression, Pharm. Anal. Acta 9 (2018).
[56] A. Almaya, A. Aburub, Effect of particle size on compaction of materials with different deformation mechanisms with and without lubricants, AAPS PharmSciTech 9 (2008) 414–418.
[57] P. Svačinová, J. Mužíková, P. Ondrejček, Comparison of compressibility, compactability, and lubricant sensitivity of two partially pregelatinized starches, Starch - Stärke 73 (2021), 2000166.
[58] A. Uzunović, E. Vranić, Effect of magnesium stearate concentration on dissolution properties of ranitidine hydrochloride coated tablets, Bosn. J. Basic Med. Sci. 7 (2007) 279–283.
[59] K. Zuurman, K. Van der Voort Maarschalk, G.K. Bolhuis, Effect of magnesium stearate on bonding and porosity expansion of tablets produced from materials with different consolidation properties, Int. J. Pharm. 179 (1999) 107–115.
[60] K.G. Pitt, M.G. Heasley, Determination of the tensile strength of elongated tablets, Powder Technol. 238 (2013) 169–175.
[61] D. Mccormick, Evolutions in direct compression, Pharmaceut. Technol. 29 (2005) 52–62.
[62] J. Cook, W. Addicks, Y.H. Wu, Application of the biopharmaceutical classification system in clinical drug development–an industrial view, AAPS J. 10 (2008) 306–310.
[63] A. Parr, I.J. Hidalgo, C. Bode, W. Brown, M. Yazdanian, M.A. Gonzalez, K. Sagawa, K. Miller, W. Jiang, E.S. Stippler, The effect of excipients on the permeability of BCS class III compounds and implications for biowaivers, Pharmaceut. Res. 33 (2016) 167–176.
[64] A. Khan, Z. Iqbal, Y. Shah, L. Ahmad, Ismail, Z. Ullah, A. Ullah, Enhancement of dissolution rate of class II drugs (Hydrochlorothiazide); a comparative study of the two novel approaches; solid dispersion and liqui-solid techniques, Saudi Pharmaceut. J. 23 (2015) 650–657.
[65] A. Nokhodchi, A. Homayouni, R. Araya, W. Kaialy, W. Obeidat, K. Asare-Addo, Crystal engineering of ibuprofen using starch derivatives in crystallization medium to produce promising ibuprofen with improved pharmaceutical performance, RSC Adv. 5 (2015) 46119–46131.
[66] Y.E. Apeji, A.R. Oyi, A.B. Isah, T.S. Allagh, S.R. Modi, A.K. Bansal, Development and optimization of a starch-based Co-processed excipient for direct compression using mixture design, AAPS PharmSciTech 19 (2018) 866–880.
[67] P.J. Jarosz, E.L. Parrott, Tensile strengths and hardness of tablets, J. Pharmaceut. Sci. 71 (1982) 705–707.
[68] N. Garg, P. Pandey, D. Kaushik, H. Dureja, Development of novel multifunction directly compressible co-processed excipient by melt granulation technique, International Journal of Pharmaceutical Investigation 5 (2015) 266–274.
[69] I. Rashid, M.M.H. Al Omari, A.A. Badwan, From native to multifunctional starch-based excipients designed for direct compression formulation, Starch - Stärke 65 (2013) 552–571.
[70] C.H. Zhang, B.X. Zhao, Y. Huang, Y. Wang, X.Y. Ke, B.J. Zhao, X. Zhang, Q. Zhang, A novel domperidone hydrogel: preparation, characterization, pharmacokinetic, and pharmacodynamic properties, Journal of Drug Delivery 2011 (2011), 841054.